

INFLUENCE OF LASER WAVELENGTH ON LASER-FIRED CONTACTS FOR CRYSTALLINE SILICON SOLAR CELLS

I. Sánchez-Aniorte^{1*}, D. Muñoz-Martín¹, M. Morales¹, P. Ortega², I. Martín², M. Colina², R. Alcubilla², C. Molpeceres¹.

¹Centro Láser UPM, Universidad Politécnica de Madrid
Ctra. de Valencia Km 7.3, 28031, Madrid, Spain, e-mail: mi.sanchez@upm.es

²Departament d'Enginyeria Electrònica, Universitat Politècnica de Catalunya
C/ Jordi Girona 1-3, Mòdul C4, 08034 Barcelona, Spain.

ABSTRACT: In the Laser-Fired Contact (LFC) process, a laser beam fires a metallic layer through a dielectric passivating layer into the silicon wafer to form an electrical contact with the silicon bulk [1]. This laser technique is an interesting alternative for the fabrication of both laboratory and industrial scale high efficiency passivated emitter and rear cell (PERC). One of the principal characteristics of this promising technique is the capability to reduce the recombination losses at the rear surface in crystalline silicon solar cells. Therefore, it is crucial to optimize LFC because this process is one of the most promising concepts to produce rear side point contacts at process speeds compatible with the final industrial application. In that sense, this work investigates the optimization of LFC processing to improve the back contact in silicon solar cells using fully commercial solid state lasers with pulse width in the ns range, thus studying the influence of the wavelength using the three first harmonics (corresponding to wavelengths of 1064 nm, 532 nm and 355 nm).

Previous studies of our group focused their attention in other processing parameters as laser fluence, number of pulses, passivating material [2, 3] thickness of the rear metallic contact [4], etc. In addition, the present work completes the parametric optimization by assessing the influence of the laser wavelength on the contact property. In particular we report results on the morphology and electrical behaviour of samples specifically designed to assess the quality of the process. In order to study the influence of the laser wavelength on the contact feature we used as figure of merit the specific contact resistance. In all processes the best results have been obtained using green (532 nm) and UV (355 nm), with excellent values for this magnitude far below 1 m Ω cm².

Keywords: Laser firing, LFC, Laser processing; Solar cell, c-Si.

1 INTRODUCTION

Laser processing of photovoltaic (PV) materials has received significant attention in the last decades [5-8]. One of the most interesting laser technologies applied in PV materials is the Laser-Fired Contact (LFC) process, in which a metal layer is laser fired through a passivating dielectric film to define ohmic contacts with the semiconductor [1-3]. In that sense this technique would replace the conventional Al-BSF (Back Surface Field Aluminium) contact formation which requires temperatures above 900 °C. In last years, LFC has been used successfully to reduce the recombination losses associated with the rear electrode, and efficiencies over 20 % have been reported on PERC (Passivated Emitter and Rear Cell) structures incorporating this technique [8, 9].

In previous studies our group has addressed the problem of a full parameterization of this process, determining the optimal frequency, pulse number, and the influence of different types of passivating materials (SiO₂, SiC_x:H(n), Al₂O₃ and SiN_x:H) in solar cell equivalent structures as a preliminary study to the incorporation of the LFC in a complete solar cell [2-4].

In the present work, we focus our attention on the influence of wavelength and laser fluences. Different Diode Pumped Solid State (DPSS) lasers emitting in their first three harmonics ($\lambda = 1064$ nm, 532 nm, 355 nm) were used.

In particular we report results on the morphology and electrical behavior of test structures using Al₂O₃ as passivating layer. Finally, we demonstrate by means of a detailed study of a particular electrical magnitude, the

specific contact resistance, that laser wavelength plays a critical role in the performance of LFC, being the electrical behavior better with shorter wavelengths.

2 SAMPLES AND EXPERIMENTAL SET-UP

The irradiation experiments were done on Al/Al₂O₃/c-Si structures specifically designed (figure 1) and described in detail elsewhere [15]. The general structure of these samples consists in <100> p-type float-zone monocrystalline-silicon wafer (resistivity 2.5 Ω cm, thickness 289 μ m) used as substrate. On the front face we deposited an Al₂O₃ film by Atomic Layer Deposition (Savannah S-300 Cambridge NanoTech) to be used as passivating layer. Thicknesses of 50 nm and 15 nm respectively for this layer has been used in this study. Next, a 1 μ m thick Al layer was deposited on top of the dielectric film. Finally, on the rear side an ohmic contact is created by depositing an Al film of 2 μ m thickness directly onto p-type c-Si back surface.

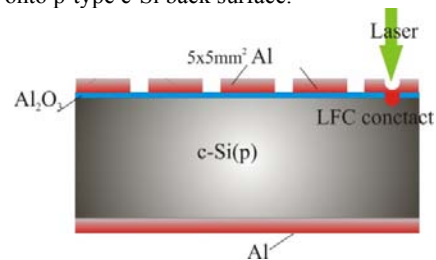


Figure 1: Diagram of the LFC process and sample structure.

In order to evaluate the electrical performance of the LFC and to obtain the specific contact resistance, a set of $5 \times 5 \text{ mm}^2$ isolated areas were prepared on the samples. In each area, a unique LFC point was done. With this approach, current-voltage characteristics (J-V) can be measured after the laser irradiation to obtain the specific contact resistance of each contacted area following the method described in previous works of the group [3, 4].

The samples were irradiated using Nd:YAG and vanadate Q-switched lasers emitting at 1064 nm, 532 nm and 355 nm, with pulse widths in the range of ns. In order to facilitate the comparison at the different wavelengths the repetition frequency has been fixed in 20 kHz and the number of pulses was kept constant to only two pulses per point in all cases. Table I summarizes the principal features of the different laser sources used in this study. The radius of the beam, ω_0 , (defined at $1/e^2$ of peak intensity) was calculated theoretically assuming a perfect Gaussian intensity profile [17].

In the case of irradiation at 532 nm and 355 nm, the beam is focused on the sample by means of an optical system formed by a digital scanner (HurryScan II 14, SCANLAB) and a lens with focal length of 250 mm. For 1064 nm, an optical beam path with a fixed focusing single lens was defined. In all systems laser power is controlled with an external energy attenuator.

Table I: Summary of Laser systems employed for Laser Firing.

λ (nm)	Model	τ (ns)	ω_0 (μm)
1064	Navigator X15SC Spectra-Physics	20	20
532	Navigator X15SC Spectra-Physics (2 ω)	15	25
355	Hippo H10-355QW Spectra-Physics	12	25

In addition, morphological characterization of laser spots was performed by using a Scanning Electron Microscopy (Hitachi S-3000N), and in-depth profiles were measured using a white light optical Confocal Leica Microscope (DCM3D). In order to get additional information regarding the compositional properties, Energy Dispersive X-ray (EDX) mapping techniques was applied to analyze the samples.

3 RESULTS AND DISCUSSION

3.1 Electrical characterization

As has been introduced before, for all the irradiation conditions we determined the specific contact resistance, ρ_c , an electrical magnitude specially well suited to assess the electrical quality of a single contact. This magnitude was calculated using the method described in reference [3], by means of the following expression:

$$\rho_c = r_{LFC} - \pi r \frac{\rho_b}{4} \quad (1)$$

where r_{LFC} is the normalized resistance of the LFC, ρ_b is the bulk resistivity and r the radius of the contact point.

To obtain the optimum parameters we have studied the sensibility of the contact resistance to the laser fluence for the different laser wavelengths in samples with two different thicknesses (50 nm and 15 nm) of Al_2O_3 (see please Figs. 2 and 3).

For films with thickness of 50 nm, fluence values in the range of 2.5-3.5 J/cm^2 give good specific contact resistance values, below 2 $\text{m}\Omega\text{cm}^2$, using only two pulses per point for all the explored laser wavelengths. Additionally the results show that for 532 nm and 355 nm excellent electrical conditions are achieved in a wide parametric window, with values far below 1 $\text{m}\Omega\text{cm}^2$, but for 1064 nm acceptable conditions are found only in a narrow band of fluence values.

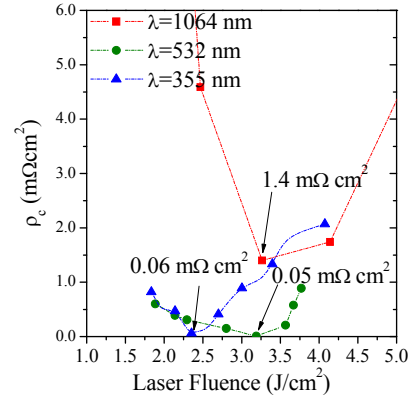


Figure 2: Specific contact resistance using different laser fluences and wavelengths in a sample with a passivating layer Al_2O_3 of 50 nm thickness.

Other relevant result is that, for this thickness of the Al_2O_3 layer, a minimum of the specific contact resistance vs fluence can be found at all wavelengths. This behavior indicates that, for these conditions, there is an optimal energy for an ideal contact formation. This behavior is probably related with the fact that the optimum LFC formation conditions are placed between two main physical regimes. First, a high laser fluence regime that cause strong Al evaporation and limits the contact formation. On the other hand, low fluence values are unable to reach the appropriate conditions of Al-Si alloy. Therefore, it is required a systematic study in order to find the optimal laser parameters.

For the samples incorporating a thinner Al_2O_3 film of 15 nm the results are shown in Fig. 3.

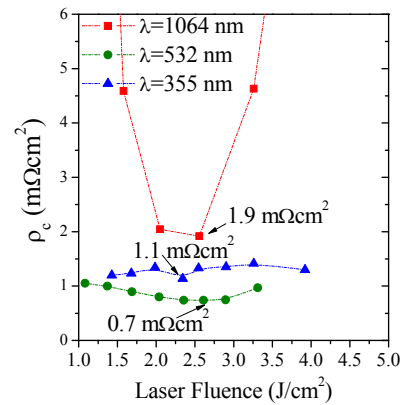


Figure 3: Specific contact resistance using different laser fluences and wavelengths in a sample with a passivating layer Al_2O_3 of 15 nm thickness.

In this case the values obtained for the specific contact resistance are slightly higher than those obtained

for the film of 50 nm. However is clearly shown that a wider parametric window is obtained for 532 nm and 355 nm with excellent values ($0.7 \text{ m}\Omega\text{cm}^2$ to $1.1 \text{ m}\Omega\text{cm}^2$), though a secondary effect to bear in mind is that, probably, the quality of the passivation is reduced by decreasing the Al_2O_3 layer.

3.2 Morphological characterization

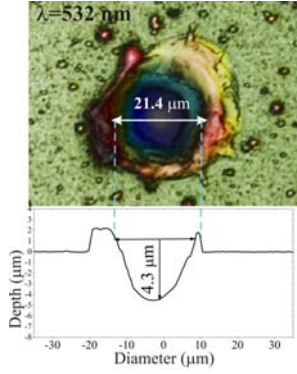


Figure 4: Confocal profile of LFC in $\text{Al}/\text{Al}_2\text{O}_3/\text{Si}$ structures at 532 nm, 20 kHz, two pulses per point, and $2.3 \text{ J}/\text{cm}^2$ (0.3 W).

A typical morphology of the obtained LFC contact is shown in figure 4. The morphology is characteristic of the interaction regime in ns, with melting of material and strong hydrodynamic effects inherent to the mainly thermal interaction processes in the ns regime at all wavelengths.

For this work, an appropriate understanding of the structural changes in the materials and the physical mechanisms of contact formation are required. For this purpose we used EDX characterization in order to determine the relative concentration of Al inside the LFC. Figure 5 shows an EDX compositional mapping in a characteristic LFC contact in which the color red is to identify the presence of Al atoms and the green one is related with the presence of Si.

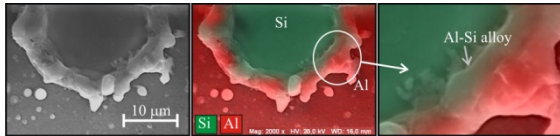


Figure 5: From left to right: SEM image, EDX color mapping and a magnified EDX image of laser-fired contact made with laser radiation of 532 nm, 2 pulses per point, and a fluence of $3.0 \text{ J}/\text{cm}^2$.

When the substrate reaches the silicon melting temperature, both silicon and aluminum forms an alloy, leading to the spot morphology observed on figures 4 and 5. This alloyed region is of the greatest importance to obtain an appropriate electrical response. It is well known that a proper Al-Si alloyed region in the edges of the contact is compulsory to assure an appropriate electrical behavior, and this effect can be observed using EDX mapping as evaluation technique.

Additionally, local diffusion of Al into Si bulk can be expected due to the inherent thermal interaction regime generated, this process is quite interesting as well due to

the p-type doping properties of Al in Si [17, 18].

The measured Al relative concentration in % as well of EDX color mapping for the optimal LFC made at three laser wavelengths are showed in figure 6. The laser fluences were chosen in function of the best electrical behavior for each LFC achieved in the following section.

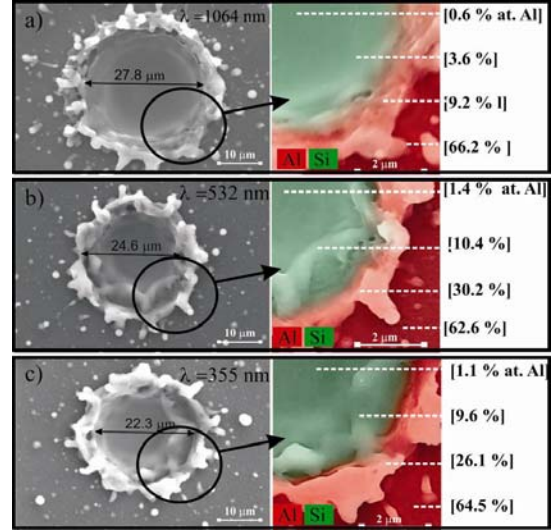


Figure 6: SEM images of laser-fired contacts on $\text{Al}/\text{Al}_2\text{O}_3/\text{Si}$ structures (left), and EDX mappings showing the relative aluminum concentration for a) 1064 nm ($3.2 \text{ J}/\text{cm}^2$), b) 532 nm ($3.0 \text{ J}/\text{cm}^2$) and c) 355 nm ($2.3 \text{ J}/\text{cm}^2$).

Indeed, from SEM/EDX inspection, it is evident that higher Al atomic concentration corresponds to the border of the crater, while the concentration decrease when we move towards the center of the generated crater. A comparison of this magnitude in the craters generated with different wavelengths shows higher concentration of Al in the case of visible radiation (532 nm). This result is corroborated with the electrical characterization discussed below, and shows that a higher content of Al atoms are beneficial for obtaining high quality ohmic contacts.

Table II summarizes the optimal laser conditions, morphological crater characteristics, specific contact resistance ρ_c and relative Al concentration in the middle of the contact crater for the three explored wavelengths.

Table II: Summary of the results obtained in this study λ represents the wavelength, d the Al_2O_3 thickness, ϕ the laser fluence, r_c is the radius of the contact, z is the depth of the contact, ρ_c specific contact resistance and [Al] the atomic Al concentration in % in the center of the generated crater.

λ (nm)	d (nm)	ϕ (J/cm^2)	r_c (μm)	z (μm)	ρ_c ($\text{m}\Omega\text{cm}^2$)	[Al]%
355	50	2.30	11.1	3.9	0.06	1.1
	15	2.30	10.5	4.2	1.10	1.0
532	50	3.00	12.3	4.4	0.05	1.4
	15	2.60	11.2	4.8	0.70	1.0
1064	50	3.20	13.9	5.6	1.40	0.6
	15	3.00	13.4	5.6	1.90	0.3

In agreement with the Table II, the best LFC conditions are achieved with the shorter wavelengths (532 nm and 355 nm) of laser radiation. Comparing the results in

Table II, it is possible to select the best laser conditions which give the lowest contact resistance.

Summarizing the results, it is clear that good electrical conditions can be found at any of the wavelength considered, being the electrical results at 532 nm and 355 nm outstanding from the point of view of the ohmic behavior. However, the authors are currently investigating a hypothesis that, in the event of being corroborated, would show that the shortest wavelength (355 nm) is preferable. The hypothesis is based on previous works of the authors [18], made only at 1064 nm, showing that this kind of laser processes induce a non negligible damage in the material probably due to thermomechanical effects generated in the interaction process. These thermomechanical processes could spoil the passivation in an area, concentric with the laser spot, greater than the visual spot in the sample. These physical phenomena are, in the case of ns interaction regime (inherently a thermal process), strongly dependent on the wavelength used. At this point authors are working in new experiments, to be published elsewhere, that would demonstrate this effect. We must point out that this effect is not detectable measuring only the specific contact resistance, so additional techniques must be used, normally implying full device characterization.

4 CONCLUSIONS

A comprehensive study about the influence of the laser wavelength on laser-fired contact (LFC) formation in solar cell structures has been presented. The study is restricted to fully commercial laser sources ready to be implemented in industrial production.

Through morphological and electrical characterization of test samples we have determined, with an appropriate parameterization, excellent conditions for LFC processes. We obtained outstanding values for the specific contact resistance ($< 1.0 \text{ m}\Omega\text{cm}^2$).

Concerning the influence of the wavelength, though in LFC formation the electrical characterization indicates similar results in contact resistance at 532 nm and 355 nm, the expected thermal affection (and potential loss in surface passivation) is less probable in UV.

To conclude, it is important to remark that a new encourage investigations are studying the development of refinements punctual back contact such as the use of punctual selective emitter before Al deposition to form the contact pattern on the back surface [18, 19].

5 ACKNOWLEDGEMENTS

This work has been supported by the Spanish Ministry of Science and Innovation under projects AMIC ENE2010-21384-C04-02/04, TEC2011-26329, TEC2008-02520 and INNDISOL IPT-420000-2010-6 (FEDER funded “Una manera de hacer Europa”).

6 REFERENCES

[1] E. Schneiderlöchner, R. Preu, R. Lüdemann and S.W. Glunz. *Prog. Photovolt: Res. Appl* 2002;
[2] I. Sánchez-Aniorte, M. Colina, F. Perales, and C. Molpeceres. Optimization of laser fired contact processes in c-Si solar cells. *Physics Procedia* 2010;
[3] P.Ortega, A. Orpella, G. López, I. Martín, C. Voz, R. Alcubilla, I. Sánchez-Aniorte, M. Colina, F. Perales, C. Molpeceres. Laser-fired contact optimization

in c-Si solar cells. *Prog. Photovolt: Res. Appl* 2011.

[4] I. Sánchez-Aniorte, R. Barrio, A. Casado, M. Morales, J.Cárabe, J.J. Gandía, C. Molpeceres. Optimization of laser-firing processes for silicon-heterojunction solar-cell back contacts. *Applied Surface Science* 2011.

[5] C. Dunsky, F., Colville, P. H., Drive, & S. Clara. Solid state laser applications in photovoltaics manufacturing. *Photovoltaics International* 2012.

[6] S.W.Glunz,E. Schneiderlöchner, D.Kray, A.Grohe, M.Hermle, H.Kampwerth, R.Preu, G.Willeke. *Proceed. 19th EU PVSEC* 2004.

[7] D. H. Neuhaus,A. Münzer, Industrial SiliconWafer Solar Cells. *Advances in OptoElectronics* 2007.

[8] A. Grohe, C. Harmel, A. Knorz, S.W. Glunz, R. Preu, *Prog. Photovoltaics Res. Appl.* 17 (2) (2009) 101–154.

[9] M. A. Green, J. Zhao, A.Wang. 23 % PV module other silicon solar cell advances'. *Proc. 2nd World Conference and Exhibition on Photovoltaic Solar Energy Conversion*, 1998.

[10] J. Zhao, A. Wang, M. A. Green. *Sol Energy Mater.Sol. Cells*,65 (1), pp. 429–435,2001.

[11] J. Martan, J. Kunes, N. Semmar. *Appl. Surf. Sci.* 253 (2007) 3525–3532.

[12] Prokhorov,A. M., Konov,V. I., Ursu, I., Mihailescu, I. N.. *Laser Heating of Metals*. Bristol, 1990, Adam Hilger.

[13] Weber,M.J. *Optics Handbook Of Optical Materials*. *CRC Press*, 2003.

[14] Bäuerle, D. *Laser Processing and Chemistry*, 3rd ed. Berlin: *Springer-Verlag* 2000.

[15] P. Ortega, A. Orpella, G. López, I. Martín, C. Voz, R. Alcubilla, I. Sánchez-Aniorte, M. Colina, F. Perales. Optimization of the rear point contact scheme of crystalline silicon solar cells. *25th EUPVSEC* 2010.

[16] Platakis, N. S. (1976). Mechanism of laser induces metal-semiconductor electrical connections in MOS devices. *J. Appl. Phys.* 2012.

[17] V.A. Bushuev, A.P. Petrakov, *Tech. Phys.* 45 (2000) 613.

[18] P. Ortega.; I. Martín, G. López, M. Colina., A. Orpella, C.Voz, R., Alcubilla. P-type c-Si solar cells based on rear side laser processing of $\text{Al}_2\text{O}_3/\text{SiC}_x$ stacks. *Solar Energy Materials & Solar Cells* 2012.

[19] M. Colina, I. Martín, C. Voz, P. Ortega, G. López, R. Alcubilla, I. Sánchez-Aniorte, C. Molpeceres. Optimization of laser doping processes for the creation of p+ regions from solid dopant sources *27th EUPVSC* 2012.